

Stellar Evolution (Single/Binaries)

Relativistic Binaries

Other Codes

Data and Code Structure



Parameterized stellar evolution tracks (single stars, $Z = 2 \cdot 10^{-2}$)

(All taken from Hurley, PhD Thesis 2000, see also Hurley et al. 2000, 2002, 2005)

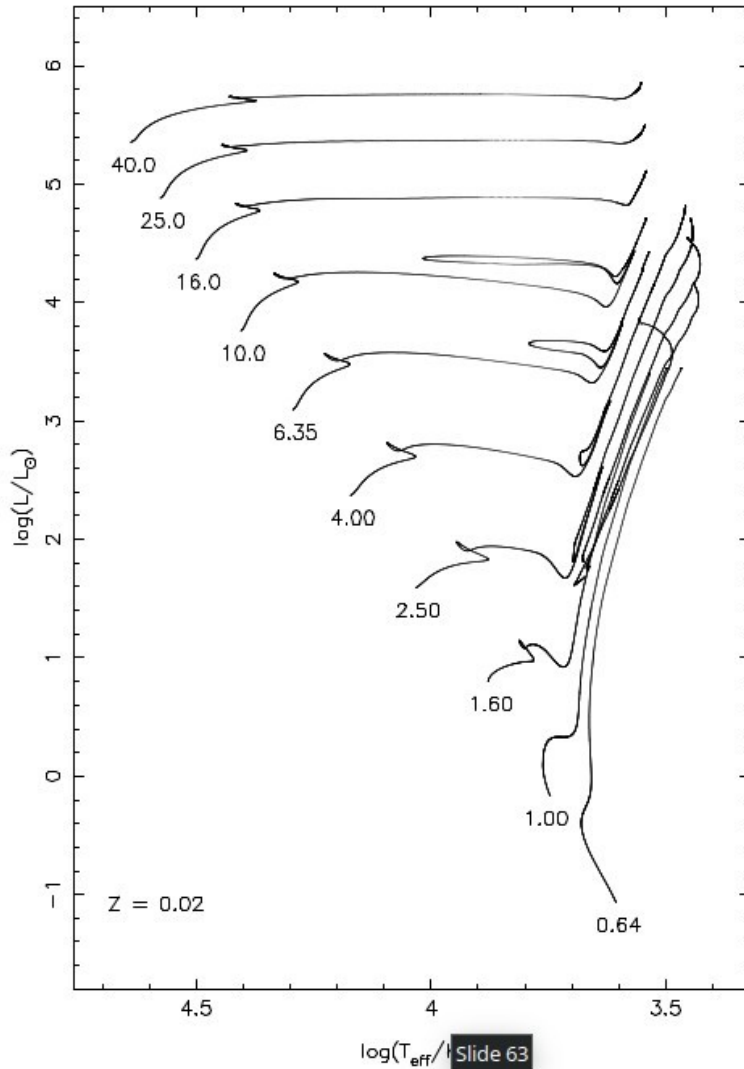


Figure 2.1: Selected OVS evolution tracks for $Z = 0.02$, for masses 0.64, 1.0, 1.6, 2.5, 4.0, 6.35, 10, 16, 25 and $40 M_{\odot}$.

SSE Single Stellar Evolution

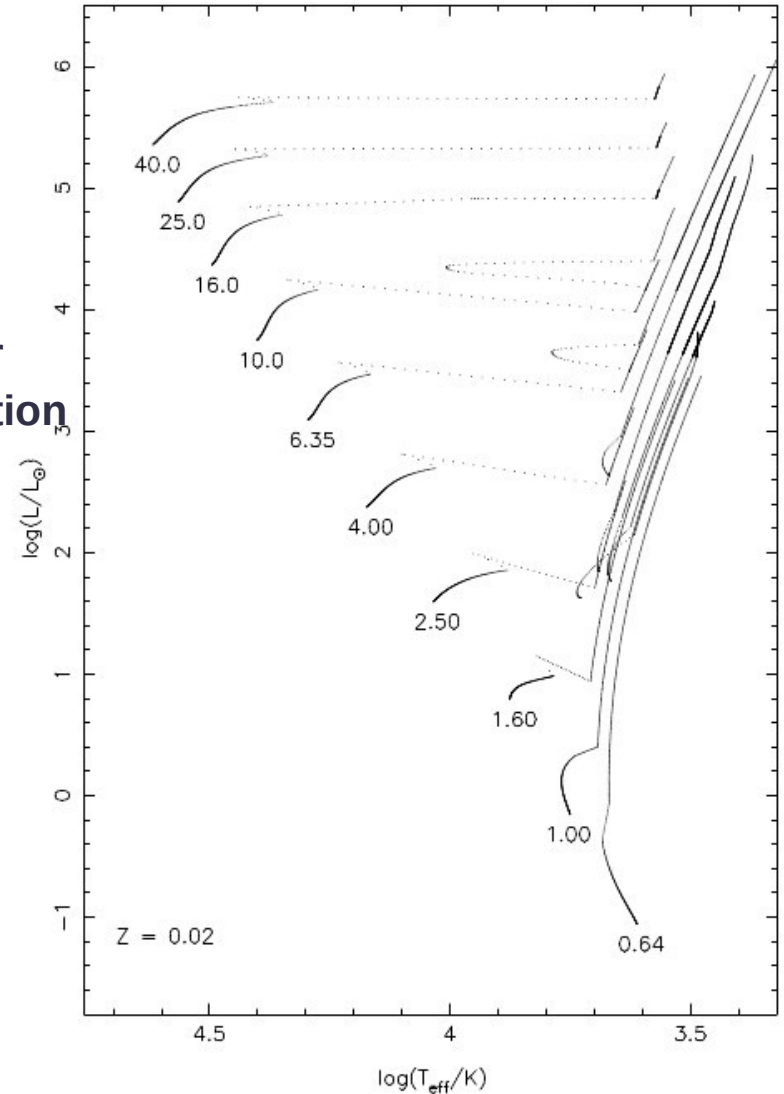
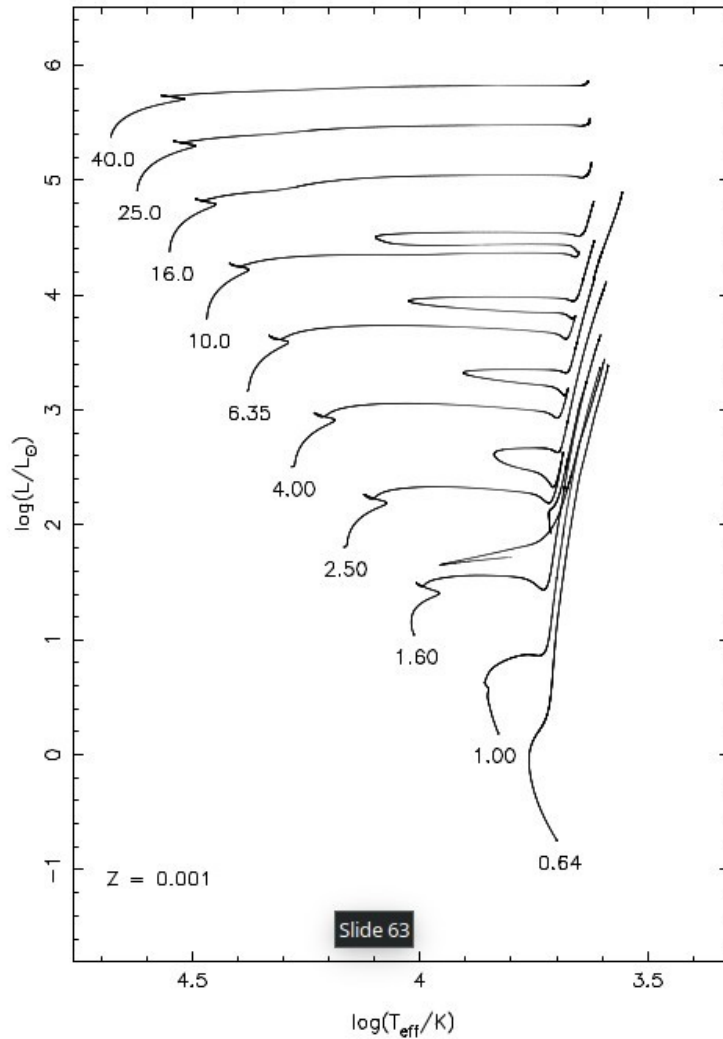


Figure 2.14: Same as Fig. 2.1 but tracks are from the evolution formulae.

Parameterized stellar evolution tracks (single stars, $Z=10^{-3}$)

(All taken from Hurley, PhD Thesis 2000, see also Hurley et al. 2000, 2002, 2005)



SSE
Single
Stellar
Evolution

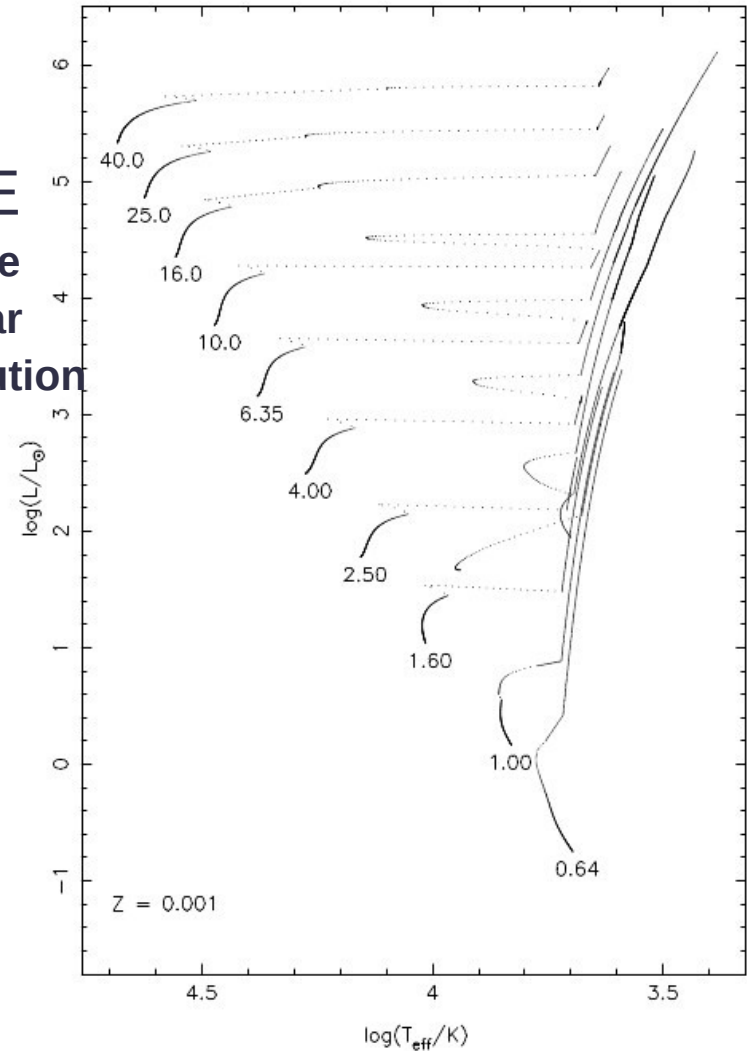


Figure 2.2: Same as Fig. 2.1 for $Z = 0.001$. The $1.0 M_{\odot}$ post He flash track has been omitted for clarity.

Figure 2.15: Same as Fig. 2.2 but tracks are from the evolution formulae.

Parameterized stellar evolution tracks (radii, different Z)

(All taken from Hurley, PhD Thesis 2000, see also Hurley et al. 2000, 2002, 2005)

SSE
Single
Stellar
Evolution

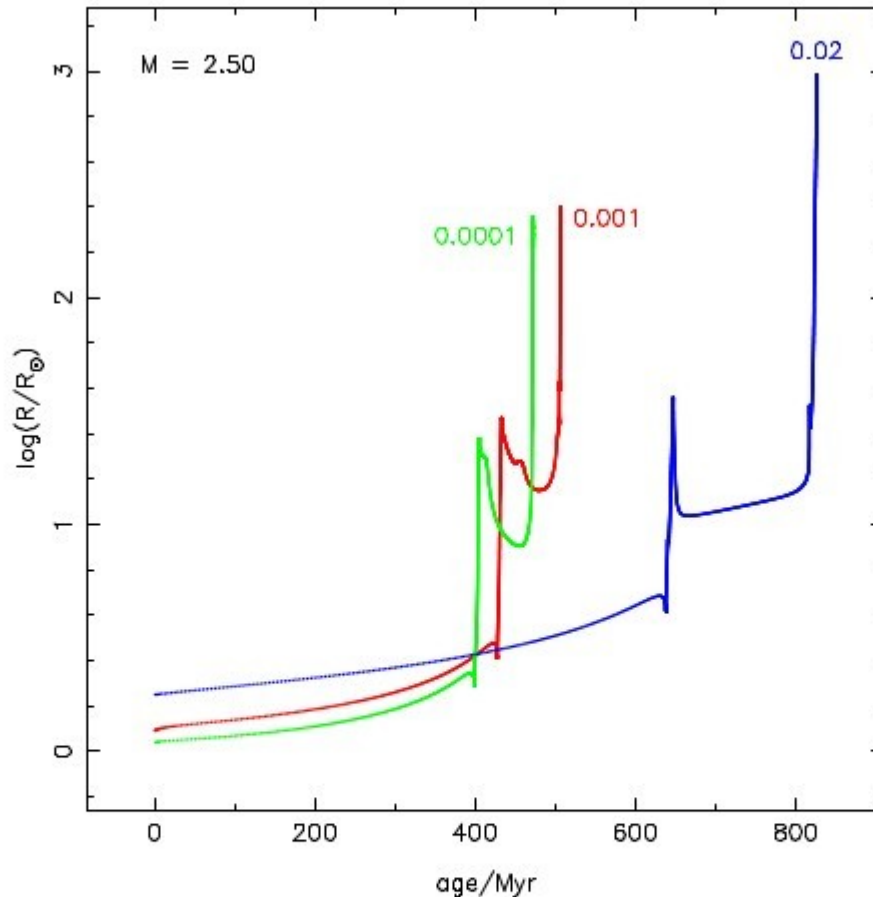
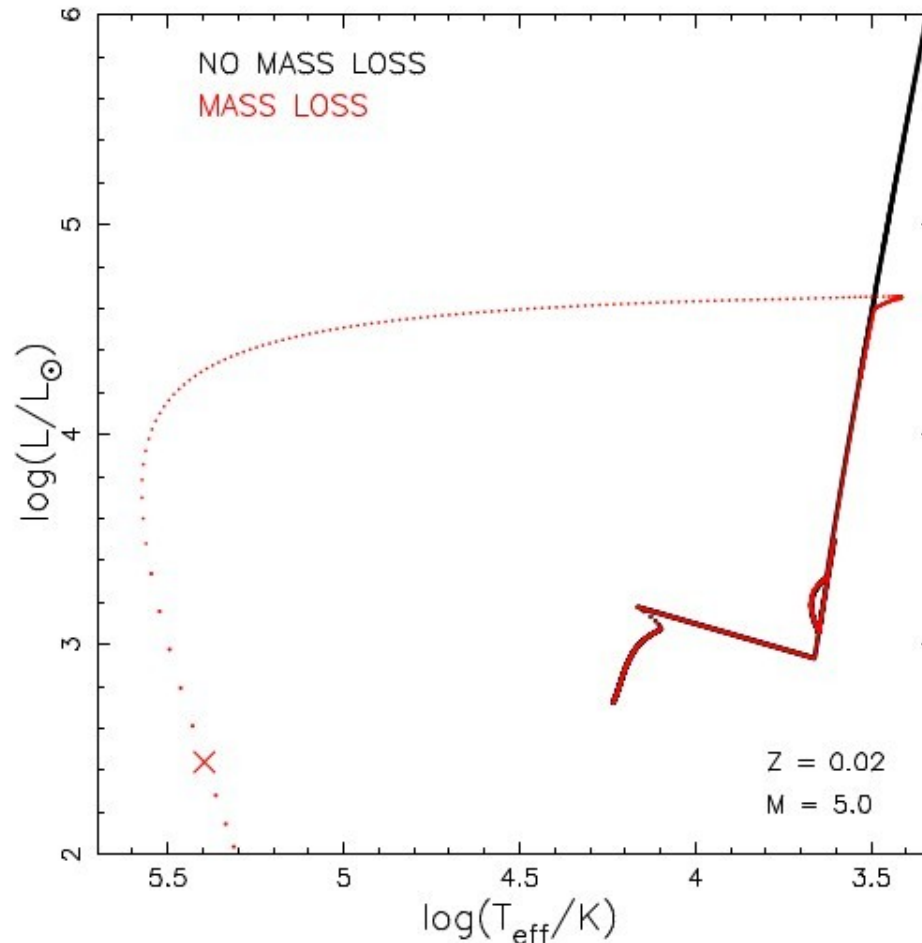


Figure 2.4: Radius evolution as a function of stellar age for $M = 2.5 M_{\odot}$, for metallicities 0.0001, 0.001 and 0.02. Track Slide 63 from the detailed models and run from the ZAMS to the point of termination on the AGB.

Parameterized stellar evolution tracks (radii, with/without wind)

(All taken from Hurley, PhD Thesis 2000, see also Hurley et al. 2000, 2002, 2005)

SSE
Single
Stellar
Evolution



Slide 63

Figure 2.16: Synthetic evolution tracks on the HRD for a $5.0 M_{\odot}$ star without mass loss (black points) and with mass loss (red points). The cross marks where the WD cooling track begins.

Parameterized stellar evolution tracks (IFMR = initial-final mass relation)

(Left: from Hurley, PhD Thesis 2000, right SSE++ from Kamlah et al. 2022)

SSE

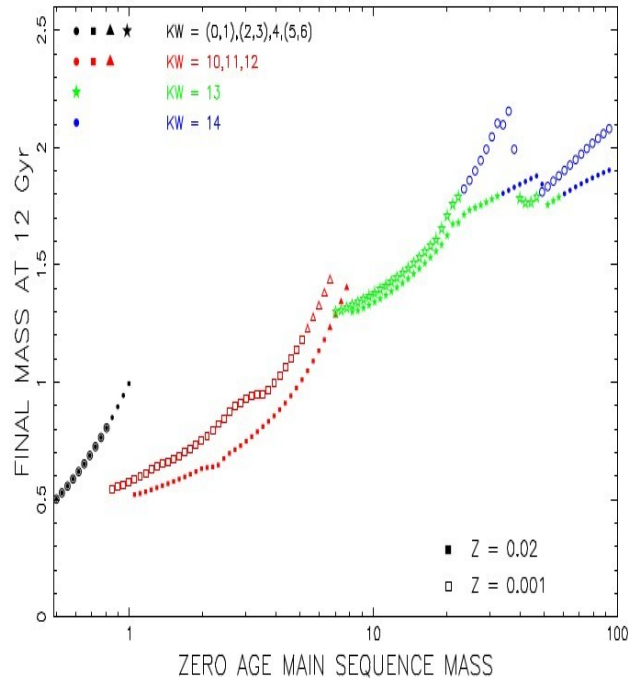
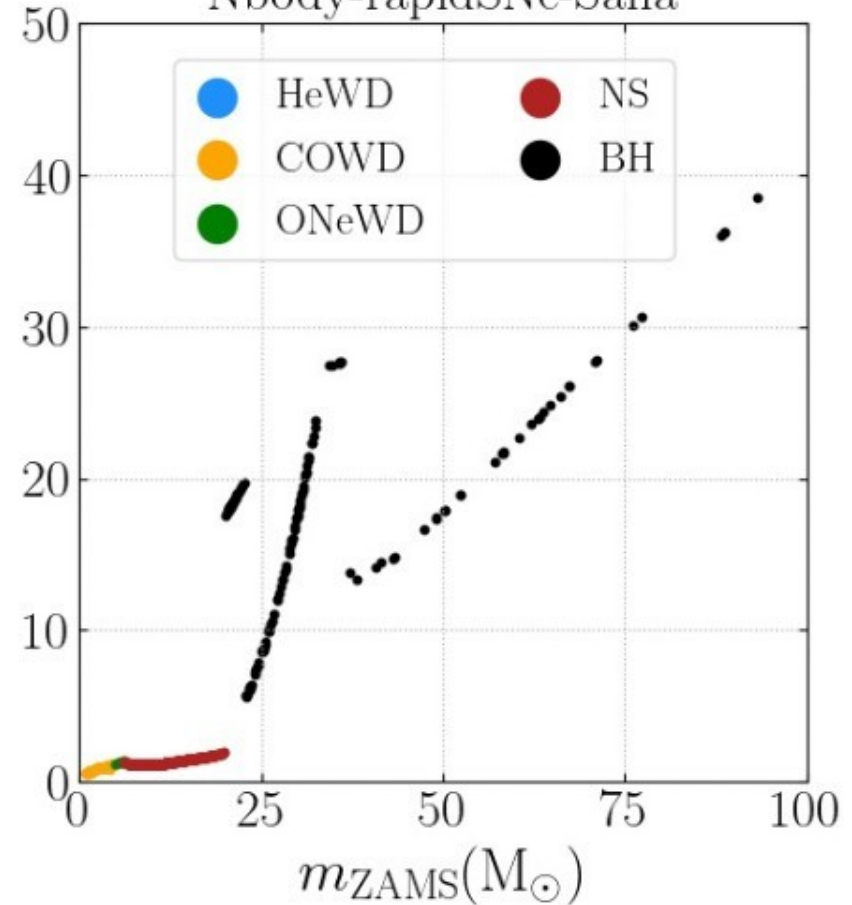


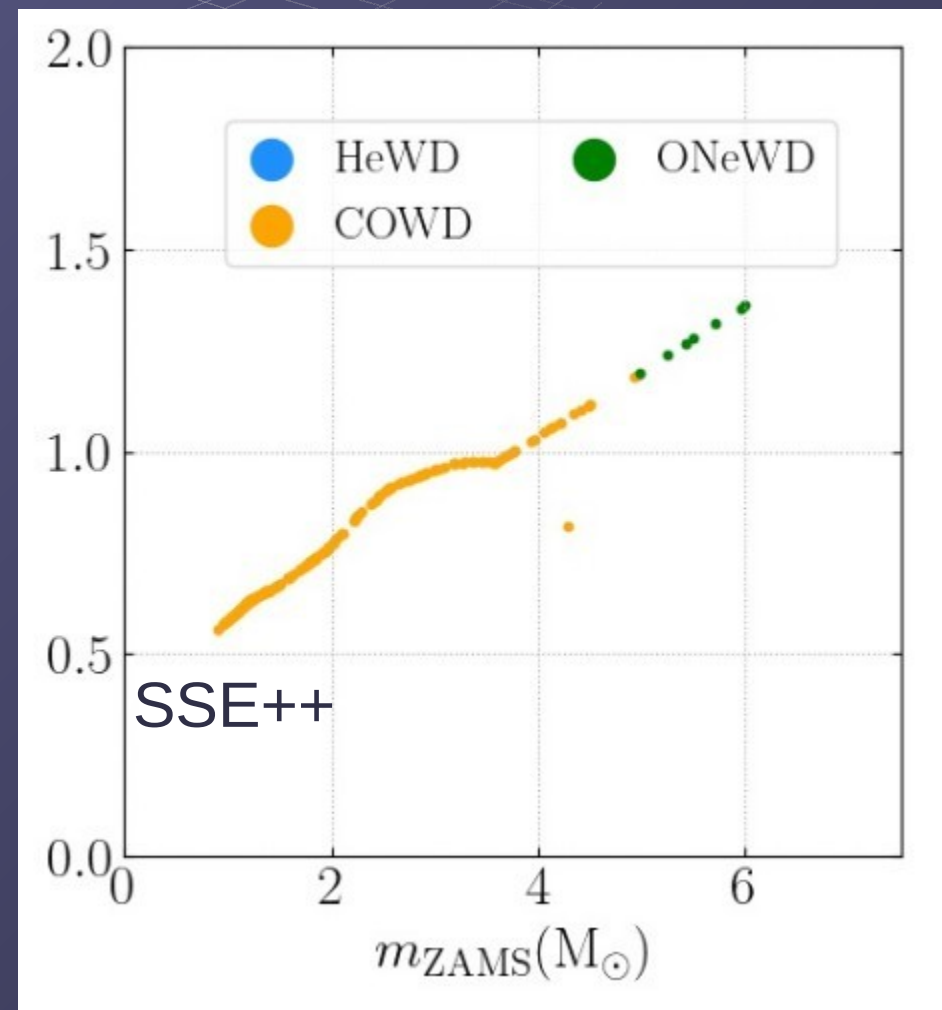
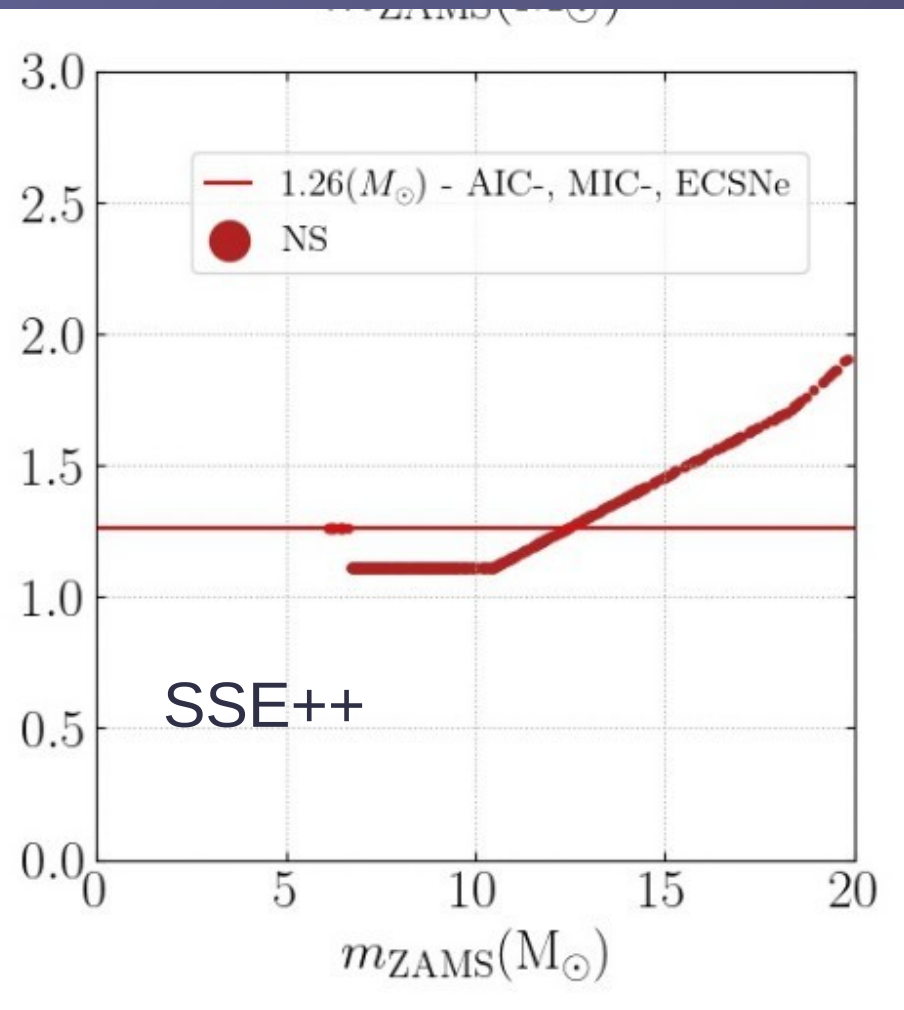
Figure 2.20: Distribution of remnant masses and types after 1.2×10^{10} yr of evolution, as a function of initial mass. $m_{\text{rem}} = 0.001$ (hollow symbols) and $Z = 0.02$ (filled symbols).

SSE++

Nbody-rapidSNe-Sana



Parameterized stellar evolution tracks (IFMR for neutron stars and white dwarfs) (SSE++/BSE++ from Kamlah et al. 2022)



Parameterized stellar evolution tracks (IFMR for neutron stars and white dwarfs) (SSE++/BSE++ from Kamlah et al. 2022)

- updated metallicity dependent core-collapse SNe, their remnant masses and fallback (Fryer et al. 2012; Banerjee et al. 2020),
- updated electron-capture supernovae (ECSNe), accretion-induced collapse (AIC) and merger-induced collapse (MIC) remnant masses and natal kicks (Nomoto 1984, 1987; Nomoto & Kondo 1991; Saio & Nomoto 1985, 2004; Kiel et al. 2008; Gessner & Janka 2018)
- (P)PISNe remnant masses (Belczynski et al. 2010, 2016; Woosley 2017),
- updated fallback-scaled natal kicks for NSs and BHs (Fuller et al. 2003; Scheck et al. 2004; Fryer 2004; Fryer & Kusenko 2006; Meakin & Arnett 2006, 2007; Fryer & Young 2007; Scheck et al. 2008; Fryer et al. 2012; Banerjee et al. 2020),
- and BH natal spins (see also Belczynski et al. (2020); Belczynski & Banerjee (2020)) from
 - Geneva model (Eggenberger et al. 2008; Ekström et al. 2012; Banerjee et al. 2020; Banerjee 2021b),
 - MESA model (Spruit 2002; Paxton et al. 2011, 2015; Banerjee et al. 2020; Banerjee 2021b),
 - and the Fuller model (Fuller & Ma 2019; Fuller et al. 2019; Banerjee et al. 2020; Banerjee 2021b).

ECSN = electron capture
Supernova

AIC = accretion induced
collapse

MIC = merger induced
Collapse

PISN = pair instability
Supernova

PPISN = pulsating PISN

NS = neutron star
BH = black hole

MESA = recent stellar
evolution model

Binary Evolution BSE (Sketched)

Taken from Hurley, PhD Thesis 2000, see also Hurley et al. 2000, 2002, 2005

$$\dot{J}_{\text{orb}} = \left[\left(\dot{M}_{1W} - \frac{M_1}{M_2} \dot{M}_{1A} \right) a_1^2 + \left(\dot{M}_{2W} - \frac{M_2}{M_1} \dot{M}_{2A} \right) a_2^2 \right] \Omega_{\text{orb}} .$$

Change of orbital angular momentum due to wind mass loss in binary

$$\dot{J}_{\text{spin}} = \left[k_2 (M - M_c) R^2 + k_3 M_c R_c^2 \right] \dot{\Omega}_{\text{spin}} ,$$

Change of spin angular momentum (convective envelope, core Mass M_c)
Equilibrium tides according to Hut (1981) – circularization

$$\frac{1}{\tau_{\text{circ}}} = \frac{|\dot{e}|}{e} = \frac{21}{2} \left(\frac{GM}{R^3} \right)^{1/2} q (1+q)^{11/6} E_2 \left(\frac{R}{a} \right)^{21/2}$$

Dynamic Tides with radiative damping (Zahn 1977)

(All taken from Hurley, PhD Thesis 2000)

Binary Evolution BSE (Sketched)

Taken from Hurley, PhD Thesis 2000, see also Hurley et al. 2000, 2002, 2005

$$\frac{\dot{J}_{\text{gr}}}{J_{\text{orb}}} = -8.315 \times 10^{-10} \frac{M_1 M_2 M_b}{a^4} \frac{1 + \frac{7}{8}e^2}{(1 - e^2)^{5/2}} \text{ yr}^{-1}$$
$$\frac{\dot{e}}{e} = -8.315 \times 10^{-10} \frac{M_1 M_2 M_b}{a^4} \frac{\frac{19}{6}e^2 + \frac{121}{96}e^2}{(1 - e^2)^{5/2}} \text{ yr}^{-1} .$$

$$\frac{|\dot{J}_{\text{mb}}|}{|\dot{J}_{\text{gr}}|} = 9.815 \times 10^9 \frac{(M_b M_1^2)^{2/3}}{M_2^2}$$

Gravitational Radiation (orbit averaged angular momentum loss and Magnetic Braking (Warner 1995)

$$\frac{R_{Li}}{a} = \frac{0.49q_i^{2/3}}{0.6q_i^{2/3} + \ln(1 + q_i^{1/3})} ,$$

Roche Lobe Overflow (Eggleton 1983)
(All taken from Hurley, PhD Thesis 2000)

Binary Evolution Relativistic (Post-Newton)

(taken from Kupi et al. 2006, Brem et al. 2013, using references below and in these papers)

$r; \mathbf{v}$: relative distance, velocity; $\mu = m_1 m_2 / M$: reduced mass ($M = m_1 + m_2$)
 $\nu = \mu / M$: mass ratio; $\mathbf{n} = \mathbf{r} / r$: unit vector in radial direction

$$\frac{dv^i}{dt} = -\frac{Gm}{r^2} [(1 + \mathcal{A}) n^i + \mathcal{B} v^i] + \mathcal{O}\left(\frac{1}{c^8}\right), \quad (181)$$

and find [43] that the coefficients \mathcal{A} and \mathcal{B} are

$$\begin{aligned} \mathcal{A} = & \frac{1}{c^2} \left\{ -\frac{3\dot{r}^2 \nu}{2} + v^2 + 3\nu v^2 - \frac{Gm}{r} (4 + 2\nu) \right\} && \text{Perihel shift} \\ & + \frac{1}{c^4} \left\{ \frac{15\dot{r}^4 \nu}{8} - \frac{45\dot{r}^4 \nu^2}{8} - \frac{9\dot{r}^2 \nu v^2}{2} + 6\dot{r}^2 \nu^2 v^2 + 3\nu v^4 - 4\nu^2 v^4 \right. && \dots \text{ higher order...} \\ & \left. + \frac{Gm}{r} \left(-2\dot{r}^2 - 25\dot{r}^2 \nu - 2\dot{r}^2 \nu^2 - \frac{13\nu v^2}{2} + 2\nu^2 v^2 \right) + \frac{G^2 m^2}{r^2} \left(9 + \frac{87\nu}{4} \right) \right\} \\ & + \frac{1}{c^5} \left\{ -\frac{24\dot{r} \nu v^2}{5} \frac{Gm}{r} - \frac{136\dot{r} \nu}{15} \frac{G^2 m^2}{r^2} \right\} && \text{Grav. Radiation} \end{aligned}$$

Schäfer, Gauge Theor. Grav. 36, 2223 (2004)

Memmesheimer, Gopakumar, Schäfer, Phys. Rev.D 70, 104011 (2004)

Blanchet, Luc; Living Reviews 2002, llr-2002-3

Binary Evolution Relativistic (Post-Newton)

(taken from Kupi et al. 2006, Brem et al. 2013, using references below and in these papers)

Spin-Orbit Interaction S / Spin-Spin SS

$$\begin{aligned} \frac{d\mathbf{v}_1}{dt} = & \mathbf{A}_N + \frac{1}{c^2} \mathbf{A}_{1PN} + \frac{1}{c^3} \mathbf{A}_S^{1.5PN} + \frac{1}{c^4} [\mathbf{A}_{2PN} + \mathbf{A}_{SS}^{2PN}] \\ & + \frac{1}{c^5} [\mathbf{A}_{2.5PN} + \mathbf{A}_S^{2.5PN}] + \mathcal{O}\left(\frac{1}{c^6}\right). \end{aligned} \quad (5.1)$$

Faye, Blanchet, Buonanno 2006

$$\begin{aligned} \mathbf{A}_S^{1.5PN} = & \frac{Gm_2}{r_{12}^3} \left\{ \left[6 \frac{(S_1, n_{12}, \mathbf{v}_{12})}{m_1} + 6 \frac{(S_2, n_{12}, \mathbf{v}_{12})}{m_2} \right] \mathbf{n}_{12} \right. \\ & + 3(n_{12} \mathbf{v}_{12}) \frac{\mathbf{n}_{12} \times \mathbf{S}_1}{m_1} + 6(n_{12} \mathbf{v}_{12}) \frac{\mathbf{n}_{12} \times \mathbf{S}_2}{m_2} \\ & \left. - 3 \frac{\mathbf{v}_{12} \times \mathbf{S}_1}{m_1} - 4 \frac{\mathbf{v}_{12} \times \mathbf{S}_2}{m_2} \right\}. \end{aligned} \quad (5.3a)$$

Rezzolla
Final Spin
Formula

$$|\mathbf{a}_{\text{fin}}| = \frac{1}{(1+q)^2} \left[|\mathbf{a}_1|^2 + |\mathbf{a}_2|^2 q^4 + 2|\mathbf{a}_2||\mathbf{a}_1|q^2 \cos \alpha \right. \\ \left. + 2(|\mathbf{a}_1| \cos \beta + |\mathbf{a}_2| q^2 \cos \gamma) |\mathbf{l}| q + |\mathbf{l}|^2 q^2 \right]^{1/2},$$

where $q = M_2/M_1$ is the mass ratio and the angles are defined as

$$\cos \alpha = \hat{\mathbf{a}}_1 \cdot \hat{\mathbf{a}}_2, \quad \cos \beta = \hat{\mathbf{a}}_1 \cdot \hat{\mathbf{l}}, \quad \cos \gamma = \hat{\mathbf{a}}_2 \cdot \hat{\mathbf{l}}.$$

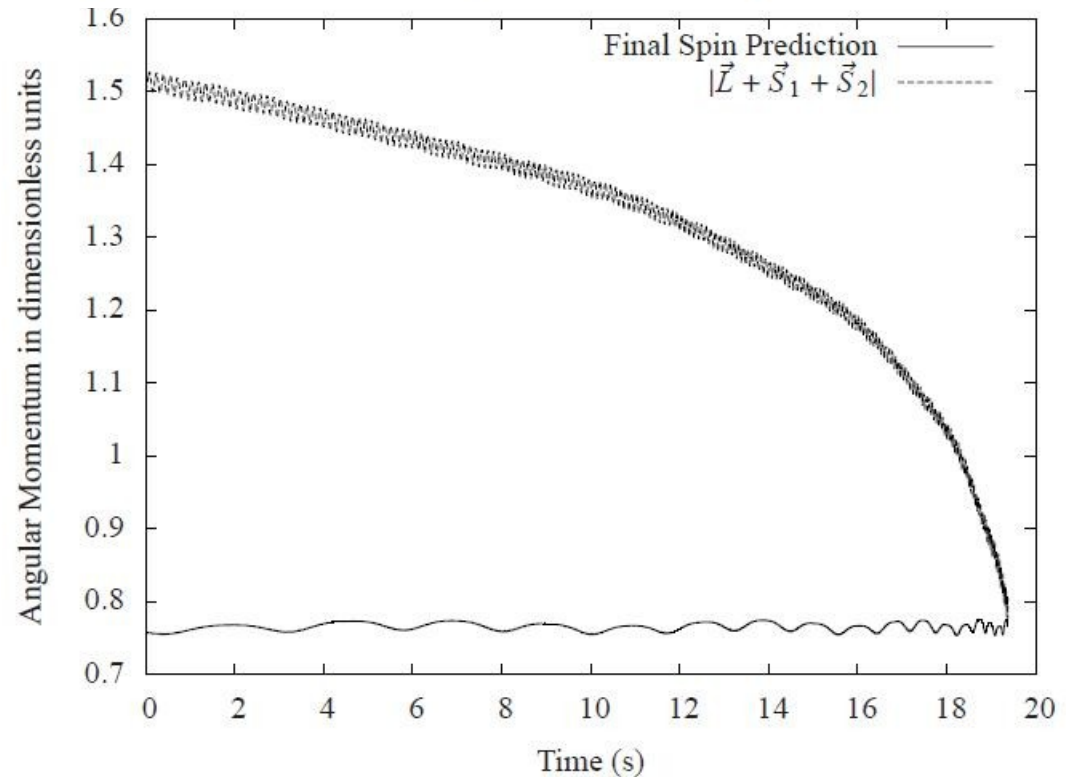


Figure 3.7: Comparison between the current final spin prediction and the actual total angular momentum of the binary system.

Brem,
Amaro-Seoane,
Spurzem,
MNRAS 2013

also

Kupi,
Amaro-Seoane,
Spurzem,
MNRAS 2006

Binary Evolution Relativistic (Post-Newton)

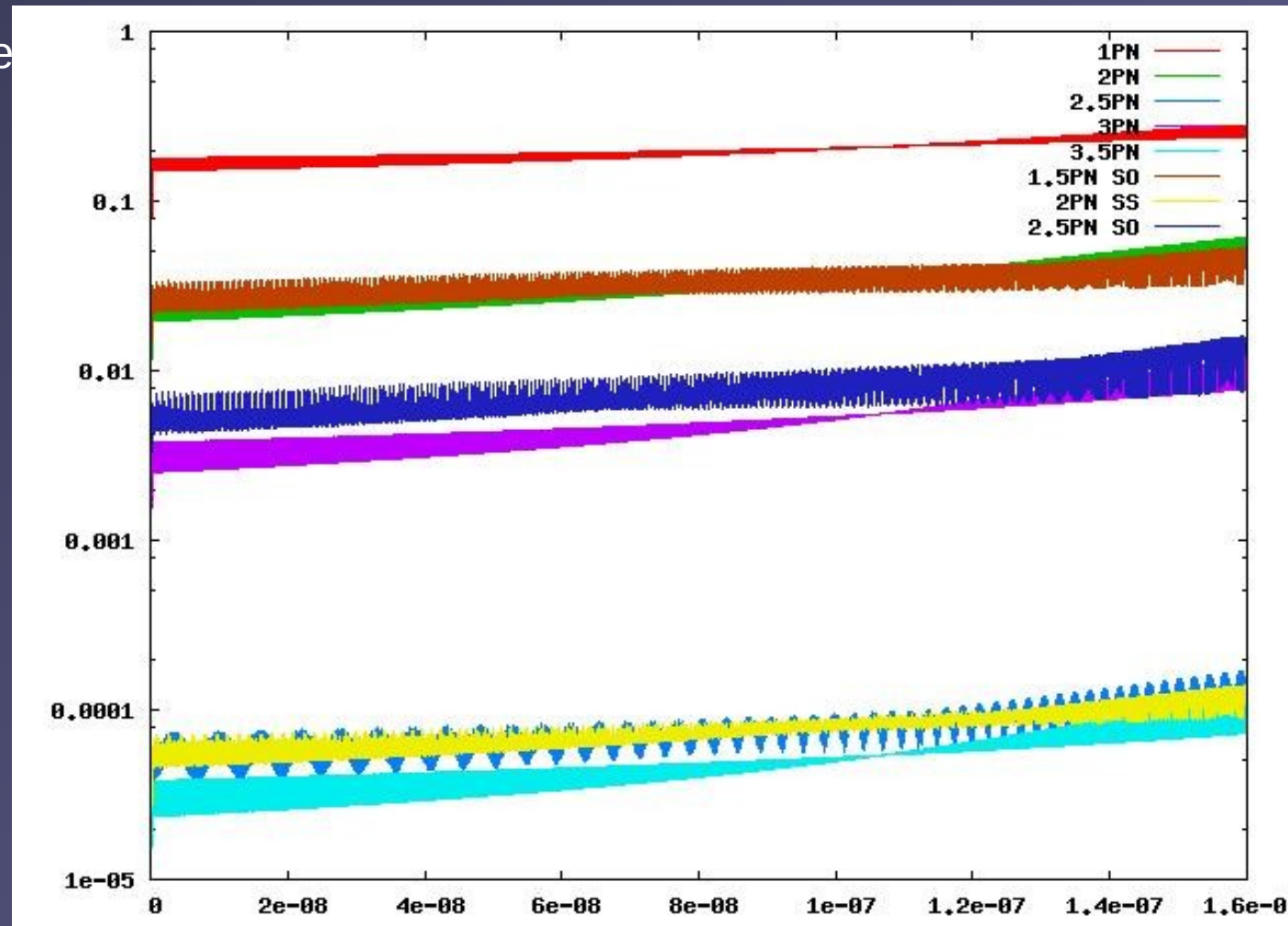
(taken from Kupi et al. 2006, Brem et al. 2013, using references below and in these papers)

Brem, Amaro-Seoane
Spurzem,
MNRAS 2013

Include
Spin-Orbit
Spin-Spin
PN3, PN3.5
Spin Dynamics

By Patrick Brem
(Diploma Thesis
Univ. Heidelberg)

1PN
2PN + 1.5PN SO
3PN + 2.5PN SO
2.5PN + 2PN SS
3.5PN



Binary Evolution Relativistic – current

(taken from Rizzuto et al. 2021, 2022, Arca Sedda et al. 2021, 2022, and DRAGONII Papers I,II,III, In preparation, using citations given here and cited in papers)

$$\left\langle \frac{da}{dt} \right\rangle = -\frac{64 G^3 m_1 m_2 (m_1 + m_2)}{5 c^5 a^3 (1 - e^2)^{7/2}} \left(1 + \frac{73}{24} e^2 + \frac{37}{96} e^4 \right),$$

$$\left\langle \frac{de}{dt} \right\rangle = -\frac{304 G^3 m_1 m_2 (m_1 + m_2)}{15 c^5 a^4 (1 - e^2)^{5/2}} e \left(1 + \frac{121}{304} e^2 \right).$$

Orbit Averaged
Post-Newtonian
(Peters & Mathews 1963,
Peters 1964)
semi-major axis a ,
Eccentricity e
(Rizzuto et al. 2021, 2022)

$$\begin{aligned} \vec{v}_{\text{GW}} &= v_m \hat{e}_{\perp,1} + v_{\perp} (\cos \xi \hat{e}_{\perp,1} + \sin \xi \hat{e}_{\perp,2}) + v_{\parallel} \hat{e}_{\parallel}, \\ v_m &= A \eta^2 \sqrt{1 - 4\eta} (1 + B\eta), \\ v_{\perp} &= \frac{H \eta^2}{1 + q_{\text{BBH}}} \left(S_{2,\parallel} - q_{\text{BBH}} S_{1,\parallel} \right), \\ v_{\parallel} &= \frac{16 \eta^2}{1 + q_{\text{BBH}}} \left[V_{11} + V_A \Xi_{\parallel} + V_B \Xi_{\parallel}^2 + V_C \Xi_{\parallel}^3 \right] \times \\ &\quad \times \left| \vec{S}_{2,\perp} - q_{\text{BBH}} \vec{S}_{1,\perp} \right| \cos(\phi_{\Delta} - \phi_1). \end{aligned}$$

Implementation of
relativistic kick after
gravitational wave
Induced coalescence
(Arca Sedda et al. 2020,
2021; following papers
cited therein)

Other Codes

(Short, no details)



MSTAR – a fast parallelised algorithmically regularised integrator with minimum spanning tree coordinates

MNRAS 2021

Antti Rantala^{1,2*}, Pauli Pihajoki², Matias Mannerkoski², Peter H. Johansson², Thorsten Naab¹

¹Max-Planck-Institut für Astrophysik, Karl-Schwarzschild-Str. 1, D-85748, Garching, Germany

²Department of Physics, Gustaf Hällströmin katu 2, University of Helsinki, Finland

BIFROST

FROST: a momentum-conserving CUDA implementation of a hierarchical fourth-order forward symplectic integrator

MNRAS 2021

Antti Rantala^{1*}, Thorsten Naab¹, Volker Springel¹

¹Max-Planck-Institut für Astrophysik, Karl-Schwarzschild-Str. 1, D-85748, Garching, Germany

Time-symmetric

4th order

New CUDA

Minimum

Spanning

Tree

BIFROST: simulating compact subsystems in star clusters using a hierarchical fourth-order forward symplectic integrator code

arxiv, subm. MNRAS 2022

Antti Rantala^{1*}, Thorsten Naab¹, Francesco Paolo Rizzuto², Matias Mannerkoski², Christian Partmann¹, Kristina Lautenschütz¹

¹Max-Planck-Institut für Astrophysik, Karl-Schwarzschild-Str. 1, D-85748, Garching, Germany

²Department of Physics, University of Helsinki, P.O. Box 64 (Gustaf Hällströmin katu 2), FI-00014, University of Helsinki, Finland

Algorithmic

Regularization

PETAR – a hybrid N-Body – Tree – Code (P³T)

A slow-down time-transformed symplectic integrator for solving the few-body problem

Long Wang^{1,2*}, Keigo Nitadori² and Junichiro Makino²

¹*Department of Astronomy, School of Science, The University of Tokyo, 7-3-1 Hongo, Bunkyo-ku, Tokyo, 113-0033, Japan*

²*RIKEN Center for Computational Science, 7-1-26 Minatojima-minami-machi, Chuo-ku, Kobe, Hyogo 650-0047, Japan*

PeTar: a high-performance N -body code for modeling massive collisional stellar systems

Long Wang,^{1,2*} Masaki Iwasawa,^{2,3} Keigo Nitadori² and Junichiro Makino^{2,4}

¹*Department of Astronomy, School of Science, The University of Tokyo, 7-3-1 Hongo, Bunkyo-ku, Tokyo, 113-0033, Japan*

²*RIKEN Center for Computational Science, 7-1-26 Minatojima-minami-machi, Chuo-ku, Kobe, Hyogo 650-0047, Japan*

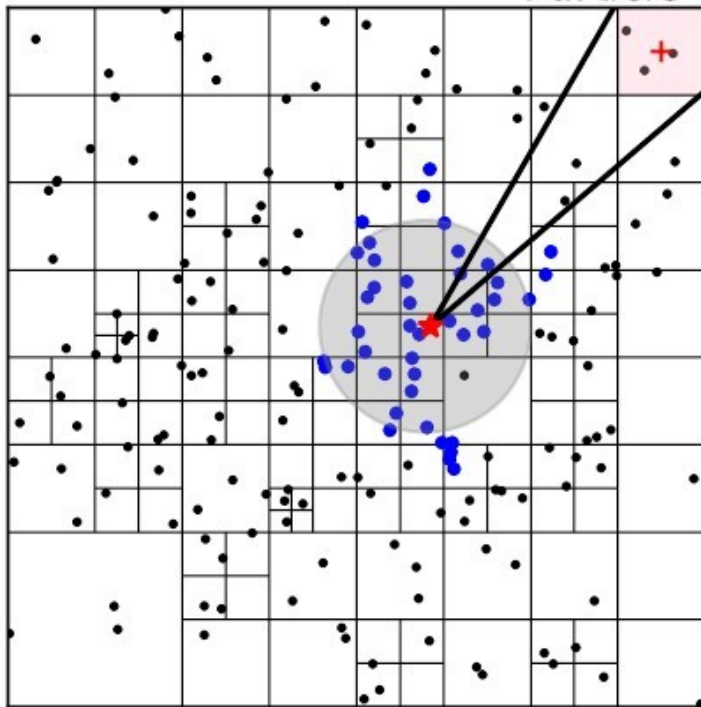
³*National Institute of Technology, Matsue College, 14-4, Nishi-ikuma-cho, Matsue, Shimane 690-8518, Japan*

⁴*Graduate School of Science, Kobe University, 1-1 Rokkodai-cho, Nada-ku, Kobe, Hyogo 657-8501, Japan*

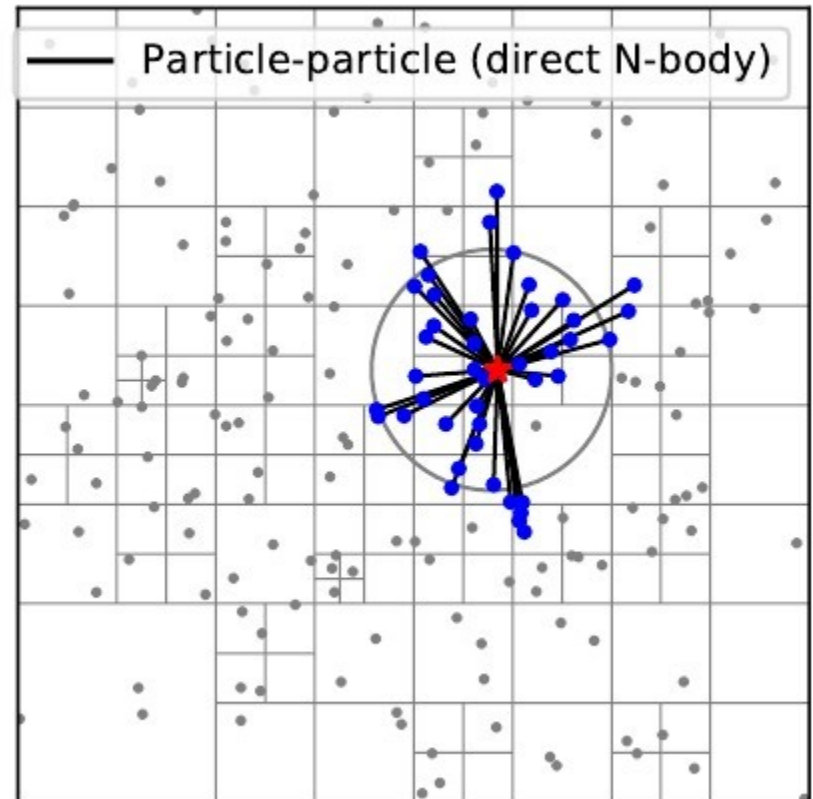
PETAR – a hybrid N-Body – Tree – Code (P³T)

long-range interaction (H_L)

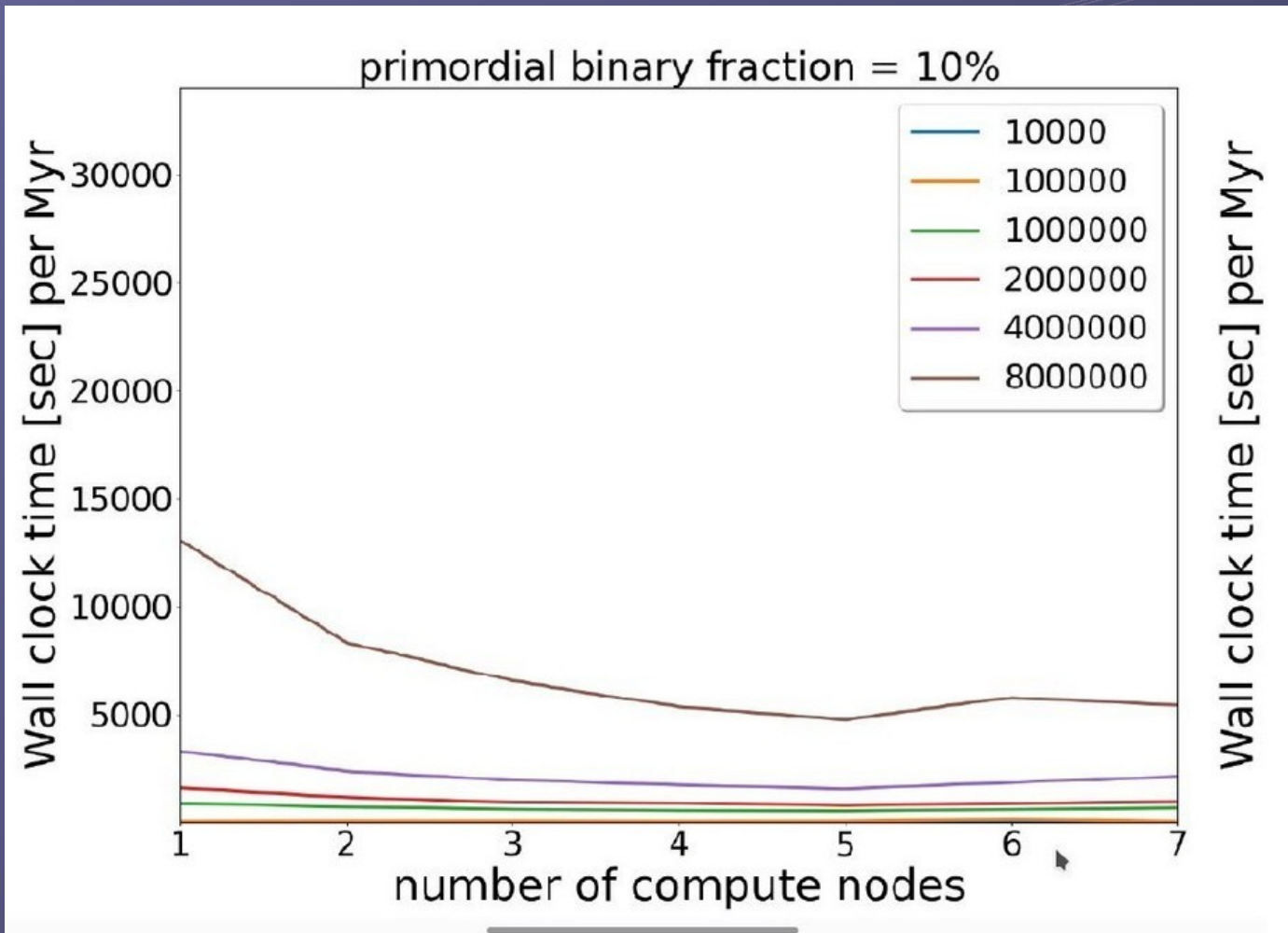
Particle-tree



short-range interaction (H_S)



PETAR – a hybrid N-Body – Tree – Code (P³T)



Strong
Scaling
Of
PeTar

On
Juwels-Booster

Ampere GPUs
1 node =
4 GPUs

(unpublished
Data from
our team with
Long Wang)

Figure 2: Scaling of PeTaR with number of nodes, 10k to 8m particles, 10% binary